UNIAXIAL AND PLANE-STRAIN COMPRESSIVE
STRENGTH OF MODEL ICE

by

G. W. Timco

(Hydraulics Laboratory, Division of Mechanical Engineering, National Research Council Canada,
Ottawa, Ontario K1A OR6, Canada)

ABSTRACT

In order to interpret reliably the results of model tests which involve compressive (crushing) failures, the compressive strength of the model ice must be known. In this paper, the uniaxial and plane-strain compressive strengths of carbamide (urea) model ice are documented for scale factors of $40 > \lambda > 5$. In addition, the influences of stress and strain-rates, platen materials and direction of loading are discussed. The results of the tests are interpreted in terms of the structure of the ice.

1. INTRODUCTION

In performing tests of dynamic ice-structure interactions in the model regime, it is important for reliable results that the mechanical properties of the model ice must be accurately scaled from those of the prototype ice. Based on Froude scaling, this entails scaling the strengths (including flexural, compressive, tensile and shear) and modulus of the ice by the linear scale factor λ of the tests while maintaining the same frictional coefficients, density and Poisson's ratio as in the prototype system. To date, the majority of tests performed in ice model-ling basins have been concerned with evaluating the performance of icebreakers operating in level-ice conditions. As such, since flexural failures predom-inate in these types of tests, attention is given to scaling the flexural strength of the ice accurately. This scaling of one strength is straightforward over a wide range of scale factors. However, with the new wave of experiments being performed in the model regime, including determining the forces exerted by a slow moving ice sheet interacting with either a rigid or a flexible structure, it is clear that scaling of only the flexural strength is no longer sufficient. In these types of tests there can be mixed mode failures which involve both flexure (bending) and compression (crushing). In addition, in several types of tests such as an ice sheet fail ing along a long straight wall, a condition of plane strain can occur. Clearly, in order to interpret reliably these types of tests, it is necessary to have a quantitative appreciation of the compressive strength of the model ice. In this paper, both the uniaxial and plane-strain compressive strengths of carbamide (urea) model ice are documented for scale factors of $40 > \lambda > 5$. In addition, the influences of loading stress and strain-rates, platen material and direction of loading are discussed. Finally, a numerical and physical comparison is made of the compressive failures of model and prototype ice.

2. STRUCTURAL PROPERTIES OF MODEL ICE

In order to have a full appreciation of the results of the compression tests, it is necessary to have a knowledge of the structure of model ice. When model ice is grown, the ice is constantly forced to grow in the supercooled regime. This creates a den-dritic structure which traps the dopant chemical between the platelets and provides the mechanisms for reducing the strength of the ice.

Before the ice is grown, the solution is mixed under cold ambient air conditions until the tempera-ture of the solution is reduced uniformly to a temp-erature $\sim 0.1°C$ above its freezing point. At this stage, agitation is stopped. With continued cooling, the upper surface of the solution becomes *thermally* supercooled so that a fine mist of water droplets (the "seeding") nucleates the surface of the water and fine ice crystals start to grow into the melt (Fig.1: layer A). Because ice is a selective lattice, it incorporates very few substitutional ions. During ice growth, therefore, the chemical dopant is mostly pushed away from the growing interface. Because of the high growth velocity for this thin ice, however, some of the chemical dopant is trapped between grain boundaries. With continuing growth, the impurities in front of the growth interface build up to an
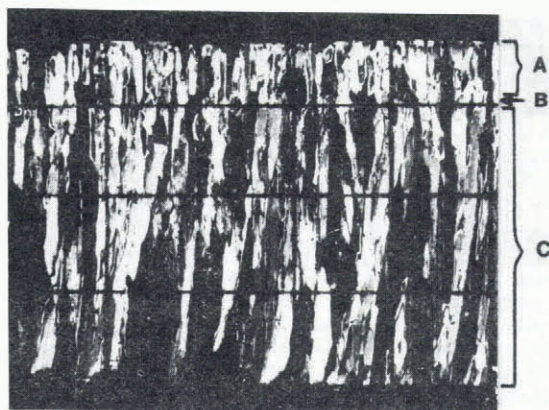
Fig.1. Vertical thin section of model ice. The grid is 1 cm on a side.

extent whereby the solution in front of the interface becomes *constitutionally* supercooled (i.e. super-cooled as a result of composition). At this stage (Fig.1: layer B), the dendritic structure becomes the stable growth phase, and the rest of the ice thickness grows with this structure (Fig.1: layer C). After the freeze, the air temperature is raised to ~+1°C to warm the ice sheet. Because of the phase relationship between urea and water, the urea trapped in the ice starts to melt the ice internally. This results in a reduction in strength of the ice which continually decreases for increasing times of warming. In this way, the strength of the model ice can be altered to produce flexural strengths which represent model scale factors between 5 and 40, depending on the time of warming.

3. UNIAXIAL COMPRESSION

In designing the tests, the mechanically weak nature of model ice presents several unique problems which influence the type of test which can be done (Timco 1981). These problems include the necessity for quickly testing the ice once it is removed from the solution (to minimize the effects of liquid drainage from the ice), the difficulty in choosing a suitable platen material to minimize end effects, and the necessity of having two different types of test apparatus to cover the whole range of loading rates applicable to model tests. Moreover, since refrigerated model ice is anisotropic, two loading directions must be studied. In the present tests, several sheets of carbamide (urea) model ice were grown in the refrigerated modelling basin in the Hydraulics Laboratory at the National Research Council of Canada (Pratte and Timco 1981). The urea-doped ice was chosen since it has a better ratio of strain modulus to flexural strength than has saline ice (Timco 1979), and several of the existing experimental ice tanks are using this ice for their model tests.

In testing, the flexural strength of the ice was measured using a cantilever beam technique and the ice piece was immediately cut to size on a band saw for the compression test. In these tests, a standard-sized ice piece of 10.5 x 3.6 x 3.6 cm was used. This size was chosen since it gives a 3:1 aspect ratio column which, for the horizontal loading, has an ice thickness (3.6 cm) which is in the range commonly used in model tests of ice-structure interaction. In trimming the thickness, the cut was always made off the bottom of the ice sheet. It should be noted that since model ice is a two-layer system, the strength may depend upon the relative proportion of each layer to the total thickness of the ice. Two different test apparatuses were used to measure the compressive strengths at two different loading rates. Since model tests which involve an icebreaker crushing ice require a relatively high loading rate, a lever-type compression tester, operated with an instrument push-pull gauge, was used. This type of tester has been used by Timco (1980) to document the compressive strength under a high loading rate of both carbamide- and saline-doped model ice over a limited range of scale factors, and by Nakajima and others (1981) in their model tests. For model tests of a slowly moving ice field interacting with a fixed structure, a much lower loading rate is required. For this, a screw-driven compression tester (Soiltest CT-405) which had a capacity of 0.05 MN and was instrumented with a load cell, was used. The output of the load cell was recorded on an X-time recorder so that both the yield load and time to failure t_f were obtained. The cross-head rate of the press was 4×10^{-2} mm s^{-1} which gives a nominal strain-rate $\dot{\varepsilon}_n$ of 4×10^{-4} s^{-1}. For the Soiltest press, three different platen materials were used: steel, masonite and bakelite. Of these three, only bakelite provided reliable results. With steel platens, the ice tended to melt when placed in contact with them, even when they were precooled.

With masonite platens, the high friction between the ice and the platens influences the results substantially. The bakelite platens proved successful since they were essentially frictionless and, because bakelite is an insulator, the ice did not melt when placed in contact with them.

The results of the compression tests were related to the measured flexural strength of the ice. This was done because the scale factor of the model tests is usually defined in terms of the scaled flexural strength and thickness of the model ice. For this paper, the defined scale factor λ is based on a conservative prototype flexural strength $\sigma_{f,p}$ for freshwater ice of 800 kPa; i.e. $\lambda = 800/\sigma_{f,m}$, where $\sigma_{f,m}$ is flexural strength at the model scale.

3.1. Horizontal loading

For horizontal loading (i.e. loading perpendicular to the direction of growth of the ice) tests were performed at both loading rates. With regard to the strength of the ice, the results are presented in Figure 2. The uniaxial compressive strength is shown as a function of flexural strength and scale factor for both loading rates. In addition, the high loading-rate values of Timco (1980) for carbamide ice and those of Sørensen (1978) and Edwards (1980) for saline ice are included. For the latter two, the loading rate is not known since no details of the test procedure were given. In the range of flexural strengths of 20 to 60 kPa (i.e. $40 > \lambda > 13$) the compressive strength is relatively independent of flexural strength, whereas in the range of flexural strengths of 60 to 130 kPa (i.e. $13 > \lambda > 6$) the compressive strength increases with increasing flexural strength. Over the range of flexural strengths from 40 to 130 kPa, the compressive strength is approximately twice the flexural strength. In general, the few published results of the compressive strength of saline model ice agree well with those of the carbamide ice.

Within experimental accuracy, the compressive strength of the model ice is independent of the strain-rate in the range investigated. For both
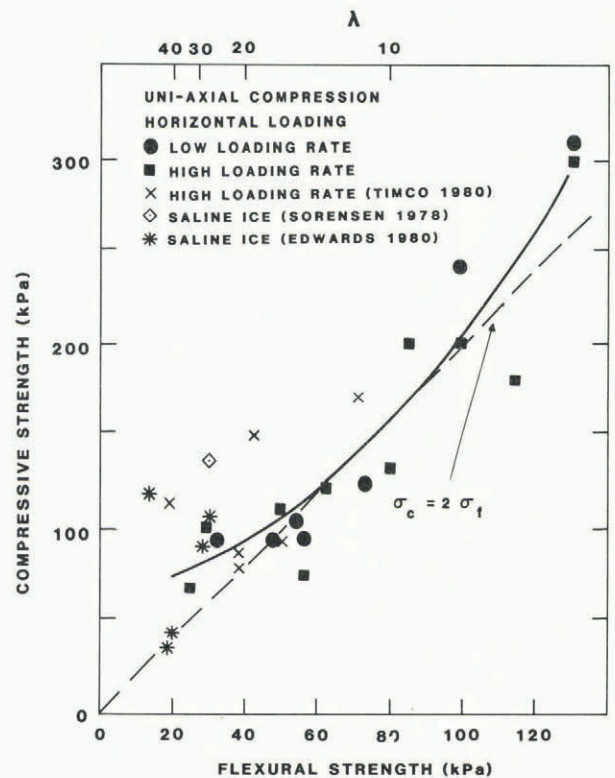
Fig.2. Horizontally loaded compressive strength versus flexural strength and scale factor.

freshwater ice and sea ice in the ductile range, the strength is dependent on the strain-rate with a functional dependence of the type $\sigma = A\varepsilon^n$ where A and n are empirically determined coefficients. Because of the independence of strain-rate for model ice, care must be taken in choosing an appropriate scale factor for the model test. For example, if the loads on an artificial island in a slowly moving ice field were being studied, the prototype strain-rate would be $\dot{\varepsilon} \approx v/2D$ where v is the rate of ice movement and D is the diameter of the island. For $v = 2.4$ m h^{-1} and $D = 100$ m, the strain-rate would be $\dot{\varepsilon} = 3.3 \times 10^{-6}$ s^{-1}. From uniaxial tests of the compressive strength of freshwater ice using a high-capacity closed-loop test machine*, $\sigma = 210(\dot{\varepsilon})^{0.34}$ (Sinha 1981) where σ is in MPa and $\dot{\varepsilon}$ is in s^{-1}. Thus, for $\dot{\varepsilon} = 3.3 \times 10^{-6}$ s^{-1}, $\sigma_{c,p} = 2.9$ MPa (note, $\sigma_{c,p}$ is compressive strength at the prototype scale). Disregarding sample-size effects, for a model test at $\lambda = 30$ (say), $\sigma_{c,m} = 97$ kPa which is in good agreement with the experimentally measured value. As such, in a test of this type, both the flexural and compressive strengths would be scaled correctly. However, it should be borne in mind that since the strength is strain-rate dependent for "real" ice, but strain-rate independent for model ice, this correct scaling of both strengths will not always be possible. Therefore, an analysis such as this is required to check on the accuracy of the scaling of compressive strength. In many cases, such an analysis will define a unique λ at which both strengths are properly scaled.

From the load-time curves from the low strain-rate tests, the average loading stress-rate $\dot{\sigma}_a$ can be determined as $\dot{\sigma}_a = \sigma_c/t_f$ where σ_c is the compressive strength of the material and t_f is the loading time to failure. The compressive strength is plotted versus the loading stress-rate for a constant strain-rate in Figure 3**. In addition, the compressive
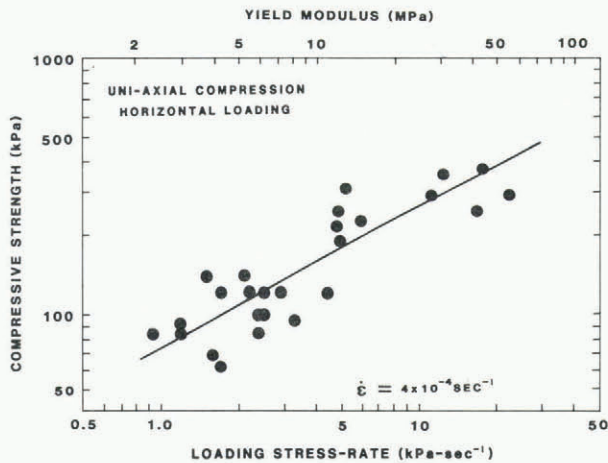
Fig.3. Horizontally loaded compressive strength versus average loading stress rate and yield modulus.

---

* The compressive strength relationship of freshwater ice is used in this example since the scale factor is defined in terms of the flexural strength of fresh-water ice. For sea ice, $\sigma_{f,p} = 500$ kPa and $\sigma_{c,p} = 30.48$ $(\dot{\varepsilon})^{0.218}$ (Wang 1979). Thus, at a model flexural strength of 25 kPa, $\lambda = 20$ and $\sigma_{c,m} = 97$ kPa, in good agreement with Figure 2.
** It should be noted that for sea ice and fresh-water ice, a graph of this type is generated by testing over a range of strain-rates. For model ice, however, this graph is generated by testing over a range of scale factors. At any one scale factor, the model ice shows no stress-rate dependence.

strength is plotted versus the yield modulus $E_n = \dot{\sigma}_a/\dot{\varepsilon}_n$ (Sinha 1982). From this log-log graph, it is evident that the compressive strength increases with increasing stress-rate such that $\sigma_c = 3.1(\dot{\sigma}_a)^{0.54}$ where σ_c is in MPa and $\dot{\sigma}_a$ is in MPa s^{-1}. Analysis of tests on freshwater ice shows a similar power-law dependence of strength on stress-rate such that $\sigma_c = 12(\dot{\sigma}_a)^{0.30}$ for freshwater ice (Sinha 1981) and $\sigma_c = 5.2(\dot{\sigma}_a)^{0.36}$ for sea ice (Frederking and Timco in press). Thus, these tests on model ice indicate that qualitatively the strength/stress-rate dependence of model ice is similar to prototype ice, but there is a stronger functional dependence for model ice.

With regard to the strain of the ice, no direct strain measurements were made. However, since the test machine is very much stiffer than the model ice, strain information can be inferred by assuming that the strain at yield ε_y in the ice is equal to the product of the nominal strain-rate $\dot{\varepsilon}_n$ and the time to failure t_f. The strain at yield and time to yield are shown versus the scale factor in Figure 4. This figure indicates that as the scale factor increases
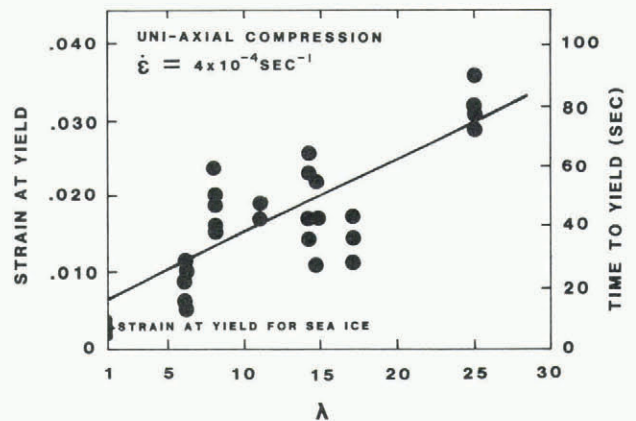
Fig.4. Strain at yield and time to yield versus scale factor for horizontally loaded uniaxial compression.

(i.e. the ice gets weaker) the strain at yield increases, such that, at the higher scale factors, there is considerable deformation in the ice before yield. Since strain is a dimensionless quantity, it should not depend on the scale factor. Rather, it should be the same for both prototype and model at any scale factor. The results of Figure 4 show that this is not the case. To see if the strain at yield at the low scale factors is in any sort of agreement with the strain at yield measurements on sea ice, a linear least-squares fit through the data was performed. Extrapolation of this fit to $\lambda = 1$ gives a strain at yield of 0.006 for model ice at that scale factor. Since the assumption made in determining the strain would tend to overestimate it, there is good agreement of this extrapolated value with the strain at yield measurements on sea ice ($\bar{\varepsilon}_y = 0.003 \pm 0.001$ (Frederking and Timco in press). This comparison indicates that at $\lambda = 1$, the strain behaviour of model ice is quantitatively similar to that of sea ice. However, as previously discussed, with increasing scale factor the strain behaviour of model ice becomes increasingly more incorrectly scaled. Overall, these tests indicate that although ice loads on structures can be well estimated in model tests, the amount of strain in the ice itself cannot.

In viewing the tests, there were two different failure mechanisms evident. In many cases, there was cracking in the sample which accelerated as the load approached the yield point until a general coalescence of the cracks weakened the internal structure and failure occurred. This is the same type of fail-

291

ure observed in ductile failures for freshwater ice and sea ice. In other cases, however, as the load was increased, the upper layer (Fig.1: layer A) and lower lower layer (Fig.1: layer C) physically split apart. With increasing load, the upper layer would buckle and crack in the centre at right angles to the direction of the load. This failure mode is not observed in small-sample tests on freshwater ice or sea ice. Clearly, the structure of the ice controls the failure behaviour of the ice.

3.2. Vertical loading

For vertical loading (i.e. loading parallel to the direction of ice growth), tests were performed only at the higher loading rate. These tests were meant to simulate the crushing behaviour of ice vertically loaded by a model icebreaker. The results of the tests are shown in Figure 5. This figure shows the vertically-loaded compressive strength as a function of flexural strength and scale factor. Included on this figure are the previous tests by Timco (1980) on carbamide ice over a limited range of conditions, and the results of Sørensen (1978) on saline ice. In general, the compressive strength increases with increasing flexural strength (decreasing scale factor) such that it is approximately 4.5 times the flexural strength. In comparing the vertically and horizontally loaded compressive strengths, it can be seen that for the lower scale factors ($\lambda < 20$) the vertically loaded compressive strength is approximately 2.3 times higher than the corresponding horizontally loaded strength. This is in good agreement with the results for sea ice. For the higher scale factors, the vertically loaded strength approaches that of the horizontally loaded strength; i.e. the ice becomes isotropic with respect to compressive strength.
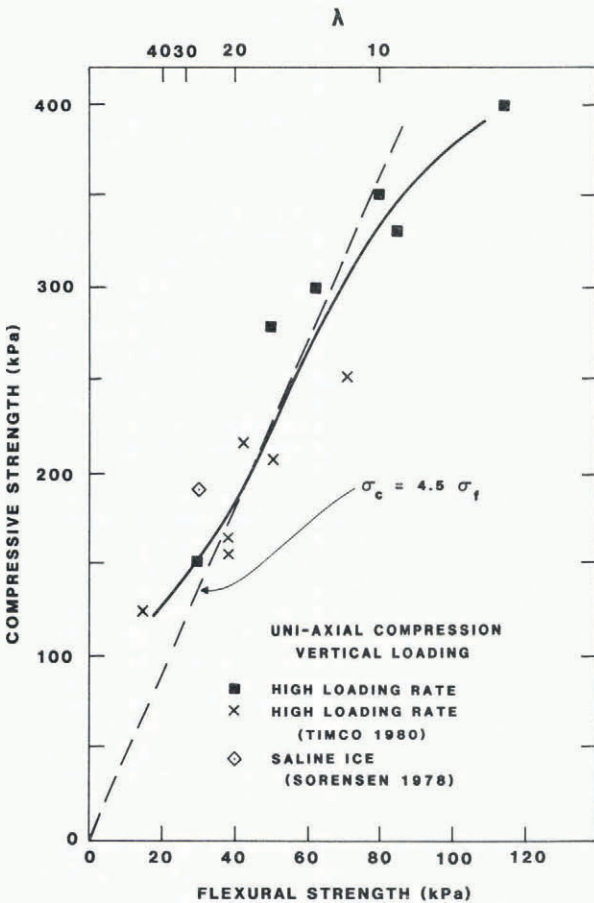
4. PLANE-STRAIN COMPRESSION

When ice interacts with a structure, it can experience a complex stress field. As such, information on the behaviour of ice under multi-axial loading is important. To date, tests of the plane-strain strength have been performed on freshwater ice by Croasdale and others (1977) and Frederking (1977), and on sea ice by Timco and Frederking (in press). In the present test series, the plane-strain compressive strength of model ice has been investigated over a range of scale factors for both Frederking type A and type B confinement conditions for one loading rate.

Plane strain has been defined as the condition where flow is everywhere parallel to a given plane and independent of position normal to the plane; i.e. there is no strain in one coordinate direction (Hill 1950). To approach this condition, a subpress was built with two parallel confining walls which restrict the ice deformation in that direction. The inside of the subpress was lined with bakelite in order to reduce the friction on the side walls. The ice samples were carefully cut to size on a band saw so that there was a tight fit in the subpress (sample size 10.5 x 3.6 x 3.6 cm). The ice was then loaded using the Soiltest press at the same rate as the uniaxial tests. For horizontal loading, confinement is possible on either the sides of the sample (A-type) or on the top and bottom of the sample (B-type). These confinement conditions are shown schematically in Figure 6.
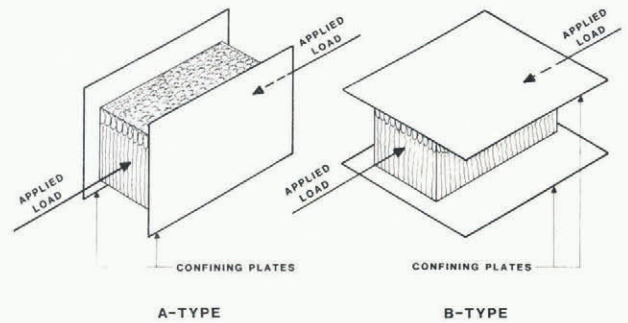
Fig.6. Schematic showing A-type and B-type confinement for plane-strain tests.

The results of the tests are presented in Figure 7, which shows the plane-strain compressive strength versus the flexural strength of the ice and the scale factor. It is evident that the plane-strain strength increases with increasing flexural strength (i.e. decreasing scale factor). In addition there is a general trend for the A-type strength to be greater than the B-type strength which is greater than the uniaxial strength of the ice. The results of tests of this type on columnar freshwater ice and sea ice have shown that the A-type strength is generally two to five times greater than either the B-type or uniaxial strengths, and that in general, the B-type and uniaxial strengths are comparable. This occurs because the predominant direction of failure for horizontal loading is in the plane of the ice cover. The A-type confinement restricts this deformation and results in significantly greater strengths (see Frederking (1977) for more detail). For model ice, a similar predominant failure direction is in the plane of the ice cover (i.e. the crack coalescence failure). As such, the side constraint of the A-type test inhibits this deformation and results in greater strengths. In most cases in the A-type test, the ice failed by separation and buckling of the two layers of the ice (i.e. the splitting failure). For the B-type tests, this splitting failure mode is prevented and the ice fails with a crack coalescence-type failure. The trend shown in Figure 7 in which

Fig.5. Vertically loaded compressive strength versus flexural strength and scale factor.
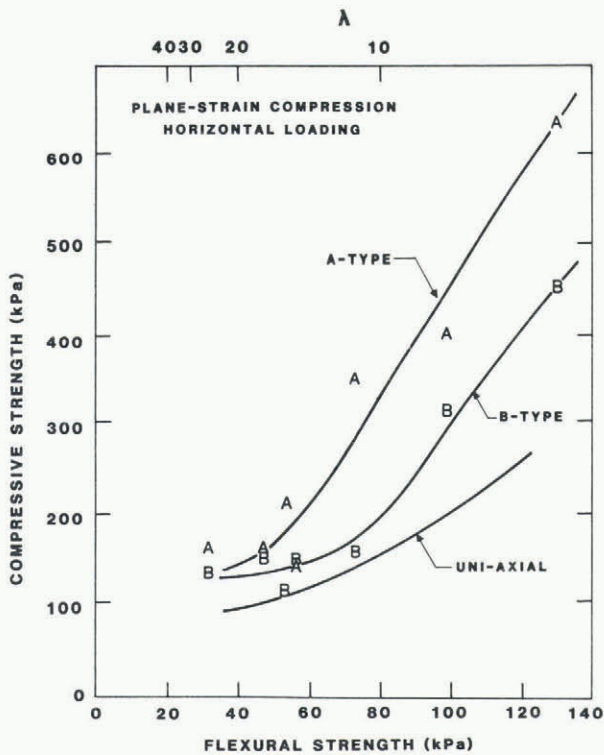
Fig.7. Plane-strain compressive strength versus flexural strength and scale factor.

$\sigma(A)>\sigma(B)>\sigma(\text{uniaxial})$ suggests that although this latter failure mode is the predominant one, the failure of unconstrained samples is influenced by both failure modes.

5. ACKNOWLEDGEMENTS

REFERENCES

Croasdale K R, Morgenstern N R, Nuttall J B 1977 Indentation tests to investigate ice pressures on vertical piles. *Journal of Glaciology* 19(81): 301-312

Edwards R Y Jr 1980 Modelling the interaction between ice and ships. *In* Tryde P (*ed*) *International Union of Theoretical and Applied Mechanics. Physics and mechanics of ice. Symposium Copenhagen ...1979 ...* Berlin, etc, Springer-Verlag: 60-81

Frederking R 1977 Plane-strain compressive strength of columnar-grained and granular-snow ice. *Journal of Glaciology* 18(80): 505-516

Frederking R, Timco G W In press. Uni-axial compressive strength and deformation of Beaufort Sea ice. *In POAC 83: the seventh International Conference on Port and Ocean Engineering under Arctic Conditions, Helsinki, 1983. Proceedings*

Hill R 1950 *The mathematical theory of plasticity.* Oxford, Clarendon Press

Nakajima H, Koma N, Inoue M 1981 The ice force acting on a cylindrical pile. *In POAC 81: the sixth International Conference on Port and Ocean Engineering under Arctic Conditions, Québec, Canada, 1981. Proceedings Vol 1:* 517-525

Pratte B D, Timco G W 1981 A new model basin for the testing of ice-structure interactions. *In POAC 81: the sixth International Conference on Port and Ocean Engineering under Arctic Conditions, Québec, Canada, 1981. Proceedings Vol 2:* 857-866

Sinha N K 1981 Rate sensitivity of compressive strength of columnar-grained ice. *Experimental Mechanics* 21(6): 209-218

Sinha N K 1982 Comparative study of ice strength data. *In IAHR. International Association for Hydraulic Research. International symposium on ice, Québec, Canada, 1981. Proceedings Vol 2:* 581-592

Sørensen C 1978 *Interaction between floating ice sheets and sloping structures.* Lyngby, Technical University of Denmark. Institute of Hydrodynamics and Hydraulic Engineering (Series Paper 19)

Timco G W 1979 The mechanical and morphological properties of doped ice: a search for a better structurally simulated ice for model test basins. *In POAC 79: the fifth International Conference on Port and Ocean Engineering under Arctic Conditions, Trondheim, Norway, 1979. Proceedings Vol 1:* 719-739

Timco G W 1980 The mechanical properties of saline-doped and carbamide (urea)-doped model ice. *Cold Regions Science and Technology* 3(1): 45-56

Timco G W 1981 On the test methods for model ice. *Cold Regions Science and Technology* 4(3): 269-274

Timco G W, Frederking R In press. Confined compressive strength of sea ice. *In POAC 83: the seventh International Conference on Port and Ocean Engineering under Arctic Conditions, Helsinki, 1983. Proceedings*

Wang Y S 1979 Crystallographic studies and strength tests of field ice in the Alaskan Beaufort Sea. *In POAC 79: the fifth International Conference on Port and Ocean Engineering under Arctic Conditions, Trondheim, Norway, 1979. Proceedings Vol 1:* 651-665

293